Beneficiation of the Nechalacho rare earth deposit. Part 2: Characterisation of products from gravity and magnetic separation

Jordens, Adam; Marion, C; Langlois, R; Grammatikopoulos, T; Sheridan, Richard; Teng, C; Demers, H; Gauvin, R; Rowson, Neil; Waters, Kristian

DOI:
10.1016/j.mineng.2016.04.007

Beneficiation of the Nechalacho Rare Earth Deposit.

Part 2: Characterisation of Products from Gravity and Magnetic Separation

Adam Jordens[1*], Chris Marion[1], Ray Langlois[1], Tassos Grammatikopoulos[2], Richard S. Sheridan[3], Chaoyi Teng[1], Hendrix Demers[1], Raynald Gauvin[1], Neil A. Rowson[4], Kristian E. Waters[1]

[1] Department of Mining and Materials Engineering, McGill University, 3610 University Street, Montreal, Quebec H3A 0C5, Canada

[2] SGS Canada Inc., 185 Concession Street, PO 4300 Lakefield, Ontario, Canada K0L 2H0

[3] School of Metallurgy and Materials, University of Birmingham, Edgbaston, Birmingham B15 2TT, United Kingdom

[4] School of Chemical Engineering, University of Birmingham, Edgbaston, Birmingham, B15 2TT, United Kingdom

*Corresponding author: adam.jordens@mail.mcgill.ca

Abstract

The application of mineral beneficiation techniques to valuable rare earth element (REE) bearing minerals requires a significant amount of research. A previous paper (Jordens *et al.*, 2015) described a series of physical separation processes employed to pre-concentrate rare earth minerals (REM) and reject iron oxide minerals from the Nechalacho Deposit. In addition to grade and recovery information it is important to understand the performance of these separations from a mineralogical perspective. Information on liberation, mineral associations, magnetic properties and size-by-size recoveries can be used to further improve process designs for this deposit.

This work employs automated mineralogy (QEMSCAN), scanning electron microscopy and a vibrating sample magnetometer to characterise the products from laboratory gravity separation (Knelson and Falcon centrifugal concentrators) and magnetic separation (varying intensity wet drum magnetic separators). The information gathered is then used to identify the optimum fraction for downstream flotation separation. The selected flowsheet included a Knelson centrifugal concentrator and low intensity drum magnetic separation resulting in a total rare earth oxide (TREO) recovery of 11.75 % and a TREO grade of 7.50 %.

Keywords: Rare Earth Elements; Gravity Separation; Magnetic Separation; Knelson Concentrator; Falcon Concentrator; QEMSCAN

1. Introduction

The characteristic properties of rare earth minerals (REM) governing their behaviour in physical separation processes such as specific gravity and magnetism are relatively well documented, however the application of this knowledge to the processing of real REM ores is not. Most REM have relatively high specific gravities (SG), as well as paramagnetic properties, suggesting that the development of beneficiation flowsheets for these minerals should begin with gravity and magnetic separation. The response of a mineral deposit to physical separation processes should always be examined from a mineralogical perspective as mineral liberation, mineral associations and the behaviour of different particle sizes can provide crucial insight into the best means of optimising the beneficiation process.

The Nechalacho REM deposit (Northwest Territories, Canada) contains many different REM as well as diamagnetic, low SG gangue minerals such as quartz and feldspar. A pre-concentration process involving multiple stages of gravity and magnetic separation has been applied to this deposit with the results described in Jordens *et al.* (2015). This work focuses on mineralogical characterisation of the separation products using a variety of tools such as automated mineralogy, scanning electron microscopy and a vibrating sample magnetometer. The resultant specific gravity and magnetic property characterisation of different product streams from this process is examined to develop an improved understanding of mineral behaviour through the different separation operations. This information informs the choice of optimum pre-concentration process.

2. Materials and Methods

2.1 Raw material

The ore used in this work originated from the Nechalacho Deposit (Avalon Rare Metals, Northwest Territories, Canada). Details regarding the operation of the various gravity and magnetic separations may be seen in Section 2 of Jordens *et al.* (2015)**.** The flowsheet of gravity and magnetic separations employed in this work may be seen in Figure 1.

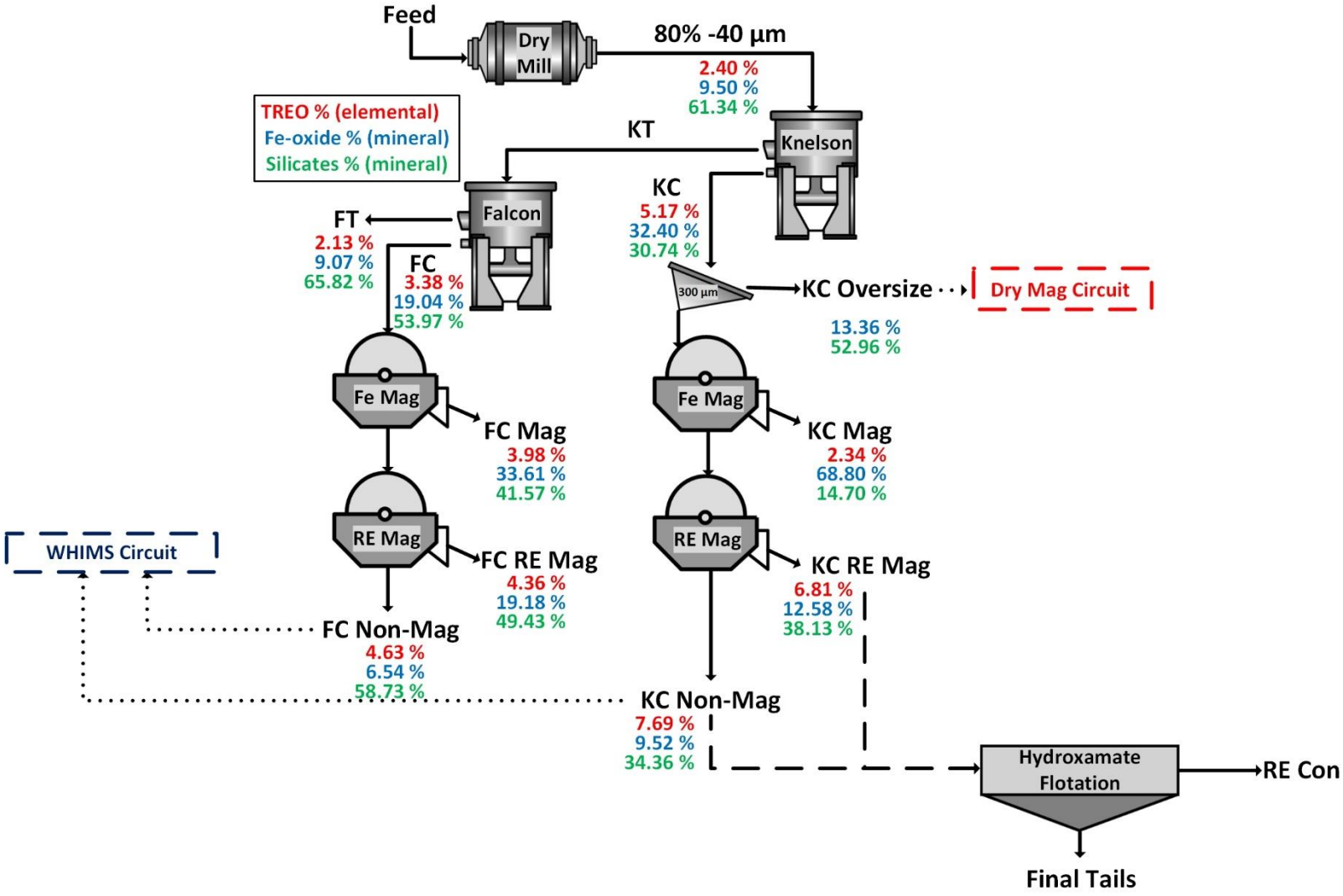

Figure 1 – Flowsheet of main gravity and magnetic separation steps applied to the Nechalacho ore after Jordens *et al.* (2015). Stream labels include grade information from ICP (TREO) and QEMSCAN (Fe-oxides and Silicates). Silicates represents the combined grade of quartz, K-feldspar and plagioclase

2.2 Mineralogical characterisation

2.4.1 Quantitative evaluation of minerals by scanning electron microscopy (QEMSCAN)

All samples used in this study were prepared as polished sections and analyzed by QEMSCAN at the Advanced Mineralogy Facility at SGS Canada (Lakefield, Canada). QEMSCAN is an EVO 430 automated scanning electron microscope equipped with four light-element energy-dispersive X-ray spectrometers and iDiscover software capable of processing the data and images. QEMSCAN operates with a 25 kV accelerating voltage and a 5 nA beam current. The QEMSCAN measures, and the iDiscover software processes, data from every pixel across a sample with a pixel size defined based on the scope of the analysis. The software assigns each pixel a mineral name based on 1,000 counts of energy dispersive X-ray spectral data and backscatter electron intensities.

If the minerals or constituent phases comprising the sample are chemically distinct, QEMSCAN is capable of reliably discriminating and quantifying minerals. Magnetite and hematite are grouped and referred to as Fe-oxides. Distinction between the two minerals when needed was conducted by optical mineralogy and X-ray diffraction (XRD) analysis. The mineral definitions were validated and refined to fit the particular samples. A reference mineral list was developed using XRD (primarily to define the major minerals), a scanning electron microscope (SEM) equipped with an energy dispersive spectrometer, and electron probe micro analysis (EPMA).

The coarse samples (>300 µm) were analyzed with the Field Image method. Chemical spectra are collected at a set interval within the field of view. Acquired data over the polished sections were conducted at a 6-20 µm pixel size. The typical diameter of a polished section was 30 mm.

The Particle Mineral Analysis (PMA) method was used for finer size samples (<300 µm). PMA is a two-dimensional mapping analysis aimed at resolving liberation and locking characteristics of a generic set of particles. A pre-defined number of particles were mapped at a 3-6 µm pixel size.

REM in QEMSCAN were identified based on their major REE. For example, monazite is defined as $(Ce,La,Nd)PO_4$. It should be noted that the QEMSCAN technique does not quantify the exact chemistry of the minerals, *e.g.*, Y in zircon or Eu in REM that occur in trace amounts. Mineral chemistry is exclusively defined by EPMA and adjusted in the software accordingly for additional calculations.

2.4.2 Electron Probe Micro Analysis (EPMA)

The compositions of the REM were determined using the wavelength-dispersive spectrometer (WDS) mode on the JEOL JXA-8900L electron microprobe at McGill University (Grammatikopoulos *et al.*, 2013).

2.4.3 Scanning Electron Microscopy (SEM)

Representative samples of each product of gravity and magnetic separation, as well as the feed, were analysed with a cold field emission SEM Hitachi SU-8230 (Hitachi High-Technologies, Canada) equipped with an XFlash 6|60 SDD (Bruker Nano GmbH, Germany) energy-dispersive X-ray spectrometer. The x-ray maps were acquired at an accelerating voltage of 15 kV with a beam current of 4 nA for one hour with a count rate of 19.3 kcps (~5% dead time). The element intensity maps were obtained with the quick deconvolution feature of the Esprit software (Bruker Nano GmbH, Germany) and qualitative phase maps were calculated with the *f*-ratio intensity method (Horny *et al.*, 2010) using a custom Python script.

2.4.4 Vibrating sample magnetometer

Vibrating sample magnetometer (VSM) measurements were conducted using a 7300 series VSM (Lake Shore Cryotronics, USA). Powder samples of <100 mg were analysed in a cylindrical VSM sample holder attached to the end of an oscillating rod. With the sample holder positioned between 4 pick-up coils and a hall probe, the rod is oscillated about a central point as a variable magnetic field is applied to produce a full hysteresis loop of -2 to 2 T (measurements taken every 0.1 T). The magnetism of the empty sample holder was measured and then subtracted from the measured data to remove this source of error. Measured magnetic moment data may then be converted to magnetisation and analysed as detailed in Jordens *et al.* (2014). In order to process the VSM data, specific gravities of each sample must be determined. These measurements were conducted using a 25 mL Gay-Lussac pycnometer (Fisher Scientific, USA).

3. Results and Discussion

3.1 Feed composition

XRD, SEM, EPMA and QEMSCAN analysis identified a number of silicates including biotite, plagioclase, quartz, K-feldspar, Fe-oxides (both magnetite and hematite), lesser proportions of muscovite/clays, chlorite, amphibole, carbonates, and trace proportions of other minerals (*e.g.*, fluorite) in the samples analysed. The REM included mainly allanite [$(Ca,Y)_2(Al,Fe,REE)_3Si_3O_{12}(OH)$], monazite [$(LREE,Y,Th)PO_4$], bastnäsite [$REE(CO_3)F$], synchysite [$Ca(REE)(CO_3)_2F$] and fergusonite [$(REE,Y)NbO_4$]. Zircon ($ZrSiO_4$) and ferrocolumbite-(Fe) ($FeNb_2O_6$) are not primary REE-bearing minerals but are important REE-Y-Nb carriers. For the purpose of this analysis, synchysite refers to solid solution synchysite and parisite.

The processed data includes information such as mineral content (wt. %), liberation and association of the minerals, grain-size, and classification of the minerals by their specific gravity among other parameters.

The mineralogy of the feed sample as determined by QEMSCAN is shown in Table 1 for the composite sample as well as the +20 µm and -20 µm size fractions. It can be seen that zircon is more abundant in the coarse size fraction. Previous work (Jordens *et al.* (2015), Section 3.1) into the elemental distribution of the feed has also reported that the coarse size fraction of the feed was enriched in heavy REE, which corresponds with the zircon abundancy as zircon is the primary host for HREE in this deposit.

Table 1 – Nechalacho deposit mineralogy (in wt. %) as determined by QEMSCAN after Jordens *et al.* (2015)

Mineral Name	Total	+20 µm	-20 µm
REM			
Zircon	7.14	9.47	5.47
Bastnäsite	0.93	1.23	0.71
Synchysite	0.55	0.27	0.75
Allanite	0.58	0.68	0.52
Columbite (Fe)	0.42	0.59	0.31
Fergusonite	0.22	0.13	0.29
Other REM	0.49	0.18	0.71
Silicate Gangue			
K-Feldspar	21.84	23.39	20.73
Quartz	20.90	19.87	21.64
Plagioclase	18.59	25.62	13.53
Biotite	13.18	5.32	18.84
Other Gangue			
Fe-Oxides	9.50	9.37	9.59
Ankerite	2.87	1.58	3.80
Calcite	0.64	0.51	0.73
Fluorite	0.55	0.46	0.62
Other Gangue	1.59	1.33	1.78

The liberation characteristics of individual particles, as well as particle associations between various minerals in the feed, were also determined from QEMSCAN analysis. Due to the complex mineralogy of the deposit, the REM containing predominantly LREE (bastnäsite, synchysite, allanite, monazite) were grouped together for this analysis and collectively referred to as light REE minerals (LREM). Figure 2 shows a summary of the liberation characteristics of the five mineral groups of interest [Fe-oxides, zircon, LREM, fergusonite and columbite (Fe)]. “Free” refers to particles with the mineral of interest having greater than 95% of the particle surface area, and “Liberated” refers to particles with less than 95% and greater than 80% of the surface area. It can be seen that for the P_{80} of 40 µm chosen in this work, liberation (“Free+Liberated”) for the iron oxides, zircon and LREM is higher than 70%, but it is lower for fergusonite and columbite. These particle mineral associations may be further broken down to include binary mixtures of a given mineral with a REM, binary mixtures of a given mineral with a gangue mineral and complex particles (“Binary-Value”, “Binary-Gangue”, and “Complex” respectively) (Figure 3). The data in Figure 3 demonstrates that many of the REM (zircon and LREM) liberate at relatively coarse (~30 µm) sizes whereas the iron oxides, and to an even greater extent fergusonite and columbite, have much smaller liberation sizes. Fergusonite is particularly fine-grained (liberation size of <15 µm), which poses additional challenges in concentrating this mineral.

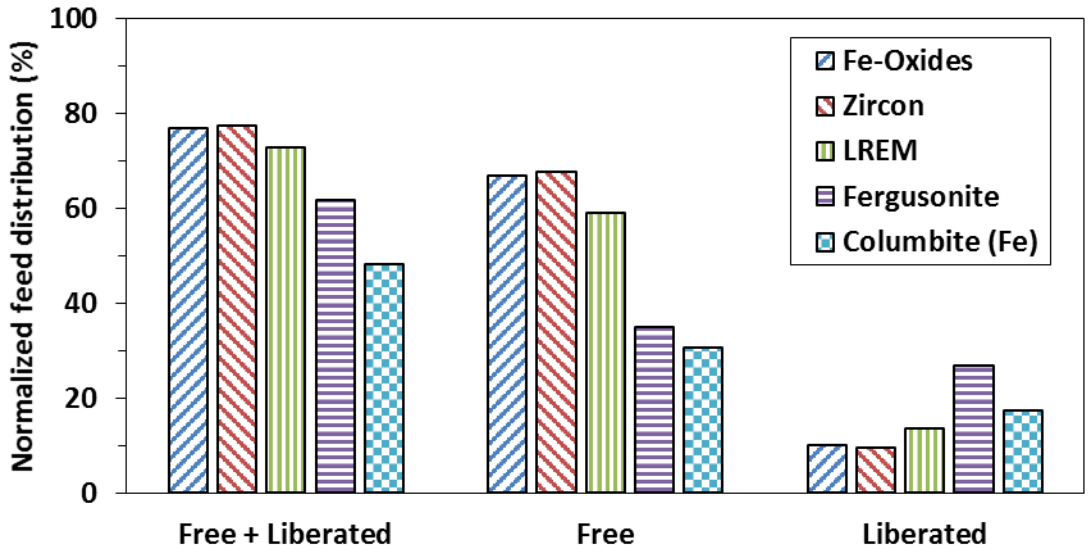

Figure 2 – Mineral liberation for the five mineral classes of interest in the Nechalacho deposit. LREM = bastnäsite, synchysite, allanite and monazite

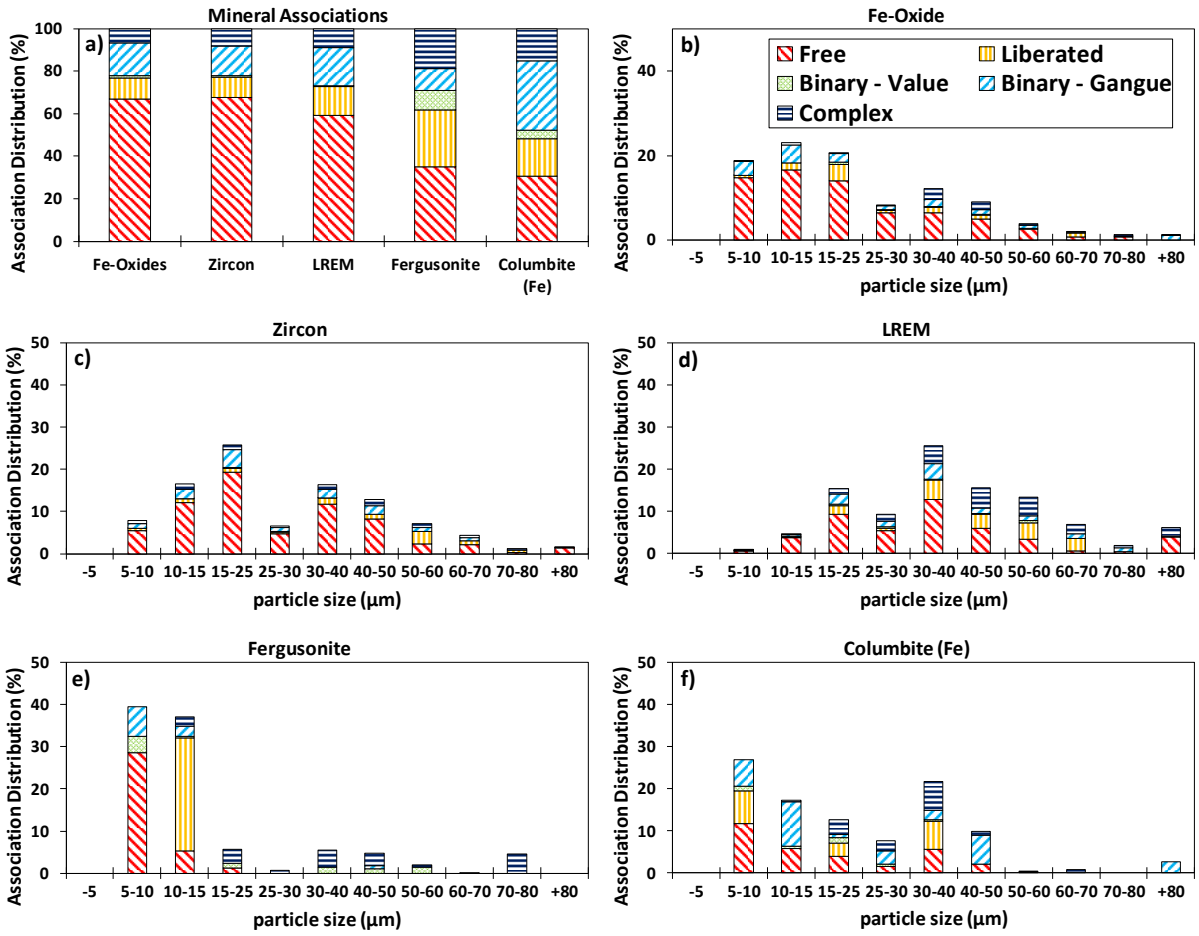

Figure 3 – Mineral associations in the Nechalacho deposit: a) total mineral association distribution for five mineral classes, b) to f) size-by-size mineral association distributions for iron oxides, zircon, LREM (bastnäsite, synchysite, allanite and monazite), fergusonite and columbite (Fe) respectively

3.2 Centrifugal gravity concentration with drum magnetic separation

3.2.1 Effect of particle size and specific gravity

The series of centrifugal gravity and drum magnetic concentration processes used for this work is shown in Figure 1. The mass pull and REO content of each different stream as well as operating conditions of both gravity separators were provided in Jordens *et al.* (2015) (Sections 2.2, 2.3 and 3.2) The d_{50} and d_{80} particle sizes (as measured by QEMSCAN) and specific gravity of each stream can be found in Figure 4, respectively. Specific gravities calculated from pycnometer measurements were determined in a similar manner to the steps found in section 10 of ASTM 854. It should be noted that ASTM 854 highlights the difficulty in applying this method to particles which may float in water, which is relevant to the present situation for very fine (< 5 µm) particle sizes which may remain at the water surface. Thus samples containing fine particles suffer from inherent measurement errors and the determined specific gravities of these fractions (-20 µm feed and all Falcon products) are likely to be slightly higher than those reported in Figure 4. The particle size and specific gravities of each fraction demonstrate that the Knelson Concentrator acts as both a size separator and gravity concentrator. The gravity concentrate from the separator (KC) has a larger particle size and elevated specific gravity (SG) relative to the intermediate tailings (KT) and

final gravity tailings (FT). The Falcon Concentrator by contrast seems to have no bias for particle size or specific gravity because the FC fraction shows little difference in particle size or SG relative to its feed (KT) and tailings (FT) streams. The mass flow rate to the Falcon Concentrator was higher than that to the Knelson with greater variability (Jordens *et al.* (2015), Section 3.2). This is to be expected as the control of mass flow rate is much easier in a lab scale when feeding dry material via a vibratory feeder (Knelson) as opposed to pumping a slurry (Falcon). A higher mass flow rate may be one factor accounting for the apparent lack of selectivity in terms of particle size or specific gravity with the Falcon Concentrator.

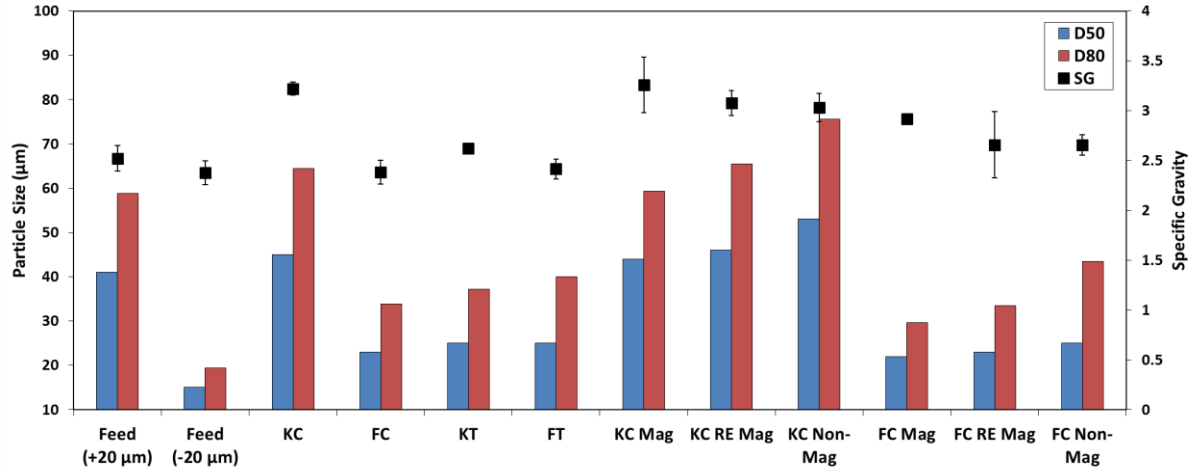

Figure 4 – Particle sizes (d_{50} and d_{80} values determined by QEMSCAN) and specific gravities of different products of centrifugal gravity concentration and drum magnetic separation. Error bars represent 95 % confidence intervals

The results of gravity separation can be better understood by using QEMSCAN data to assess recoveries of individual particles sorted by either size or specific gravity (SG). This is possible by associating an SG value to each mineral in the deposit and then calculating the SG of each measured particle as a function of the different mineral phases in the particle. The volumetric composition of a particle is estimated from the two dimensional phase map of the particle as well as stereological corrections in the QEMSCAN software (Pascoe *et al.*, 2007). The particle SG is then calculated from the volumetric composition of the particle and the specific gravities of each mineral phase. Thus, it is possible to evaluate the recoveries achieved by both the Knelson and Falcon Concentrators by SG and size class. For this purpose the particles were split into 10 size classes from 5-10 µm up to +80 µm; and 18 different SG classes from <2.5 to >6.5. The resolution limitations of this technique must be acknowledged as particles of very fine sizes will have assigned specific gravities less than the lowest possible mineral SG (~2.6 for silicates). This is because the mounting material is assigned a specific gravity of 2 such that pixels at the interface of the mineral particle will have an assigned specific gravity that is lower than that of the actual mineral phase present on the surface of the particle. Thus, for very small particle sizes these “surface” pixels contribute significantly to the overall particle specific gravity and produce particles with lower SG values than would realistically be possible for this mineral system. Additionally, particles which appear to be entirely one phase may have a lower than expected SG. In the case of zircon, bulk zircon pixels are assigned a SG of 4.6 however surface pixels which represent both mounting material and mineral are assigned a SG value of 2.

A composite view of the distribution of SG across the various size fractions in the feed material is shown in Figure 5. It can be seen that at very fine size ranges there are more particles of low SG (<2.5) and high SG

(>5.0), while at the coarsest particle sizes (+80 µm) the SG of all particles is 2.5-5. This is a reflection of the fine grained nature of the REM as the coarsest particles contain both high and low SG mineral phases.

A comparison of the total (Knelson + Falcon) gravity recovery at the fine and coarse particle sizes is illustrated in Figure 6. It is noted that there are certain categories of grouping particles by SG and size in which there are no corresponding feed particles. That is, if a distribution of particle sizes and SGs is divided arbitrarily in sufficiently small intervals, some of the intervals will contain no particles. Therefore, the zero recoveries shown are actually due to the lack of particles and not due to a lack of recovery. For example, Figure 6b shows that there are no particles of coarse size (>60 µm) in the feed, which have a particle SG within the range of 4.75-5.00 or 5.25-5.50. It is clear from Figure 6 that coarse particle recovery, even at low particle SG, is quite high, whereas fine particles (<15 µm in diameter) have very low recoveries (as would be expected). The gravity recoveries for each separator are compared in Figure 7 for small (<30 µm) particle sizes to compare the efficiency of fine particle collection between the two centrifugal gravity concentrators. The Knelson concentrator shows a clear size effect across all particle SGs, where recovery drops off dramatically with decreasing particle size. Additionally, the values for recovery of 15-30 µm particles increase significantly with increasing SG indicating that the Knelson concentrator is selectively concentrating high SG material. This effect is much less evident for the Falcon concentrator (Figure 8b), where recoveries show a very minimal increase with increasing SG and a much less pronounced decrease in recovery with decreasing particle size. This reinforces the conclusions from Figure 4 that the Falcon concentrator in this process shows very low selectivity.

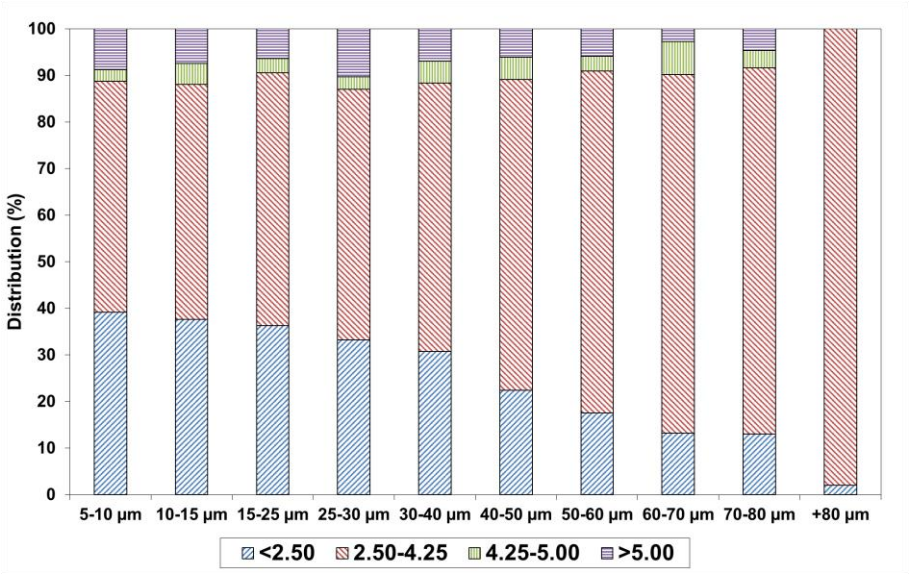

Figure 5 – Normalized distribution of particle specific gravities across different feed size fractions. The legend entries refer to particle specific gravity

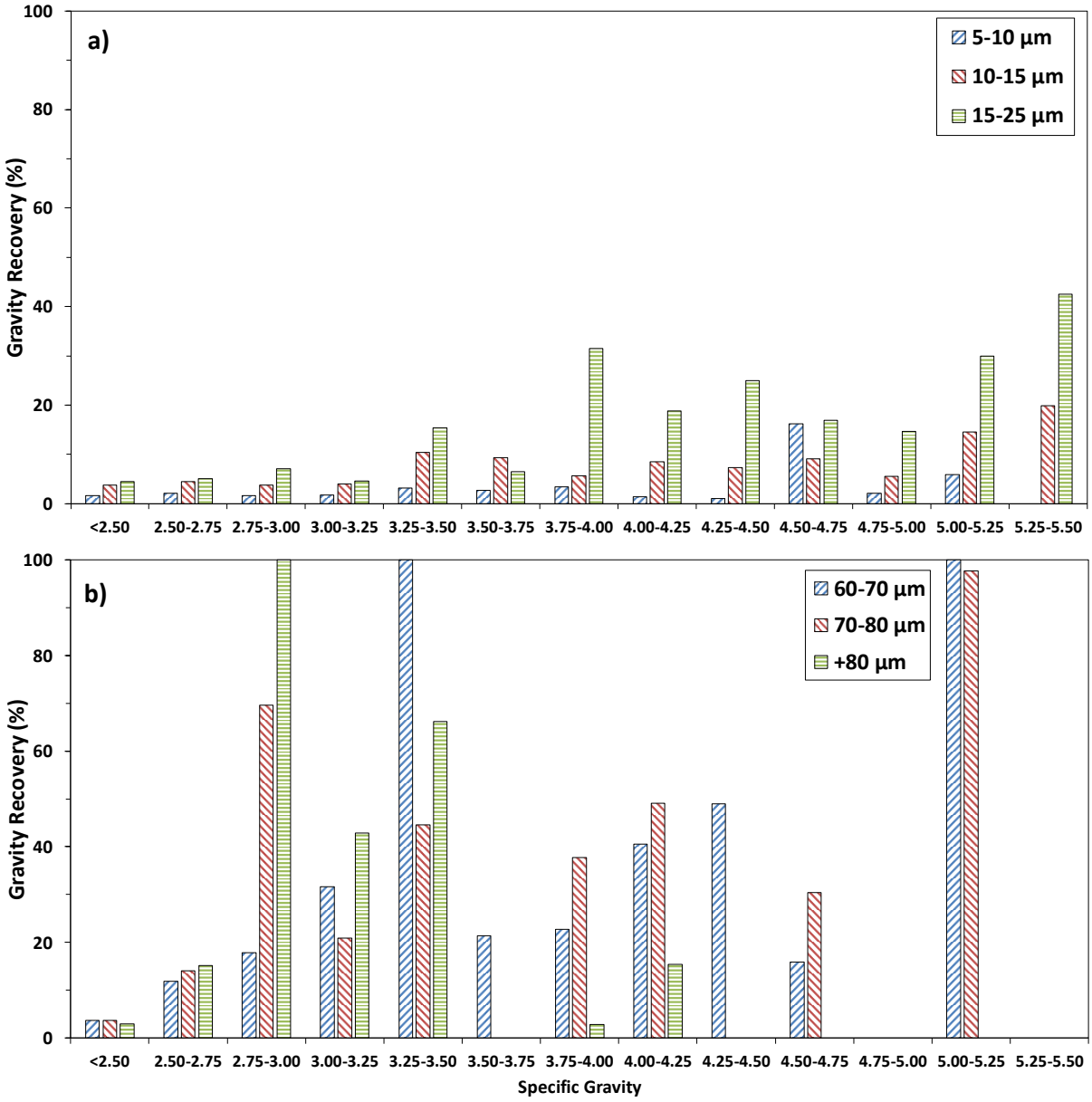

Figure 6 – Comparison of total gravity recovery (Knelson + Falcon) across particle specific gravity size classes for a) fine particle sizes and b) coarse particle sizes

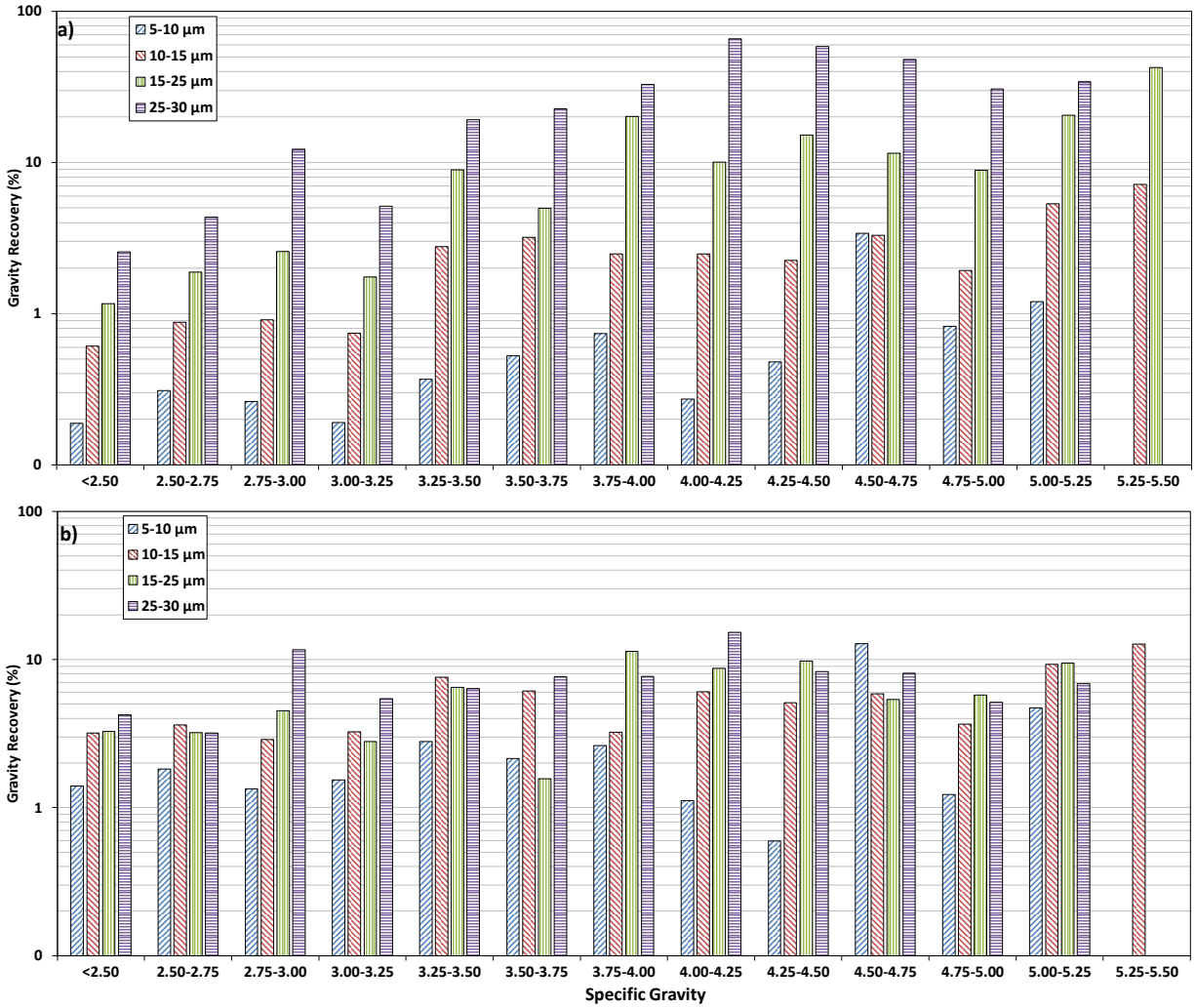

Figure 7 – Gravity recovery for small (<30 µm) particles across particle specific gravity size classes for a) Knelson gravity concentrate and b) Falcon gravity concentrate

The particle size and SG information can be filtered by the mineral phases contained in a given particle in order to evaluate the distribution of particles contained in a specific mineral across size classes (Figure 8). The Knelson and Falcon gravity concentrates were compared using the distribution of iron oxides, zircon and all particles across all size classes at 3 different SG levels. A more visual representation of this information is provided by QEMSCAN particle maps for the three same SGs (Figure 9). These two figures confirm the finding that the Knelson Concentrator in this process configuration has preferentially concentrated the coarser particles (independent of particle SG). Furthermore, zircon recovered in the Knelson gravity concentrate is well liberated at a particle SG of 4.25-4.50 (higher zircon recoveries for particles of this SG) (Figure 8 e, f), whereas in the Falcon gravity concentrate zircon recovery is primarily due to the recovery of high SG (5.0-5.25), mixed mineral particles. This inference is confirmed by the particle maps shown in Figure 9 (c, d).

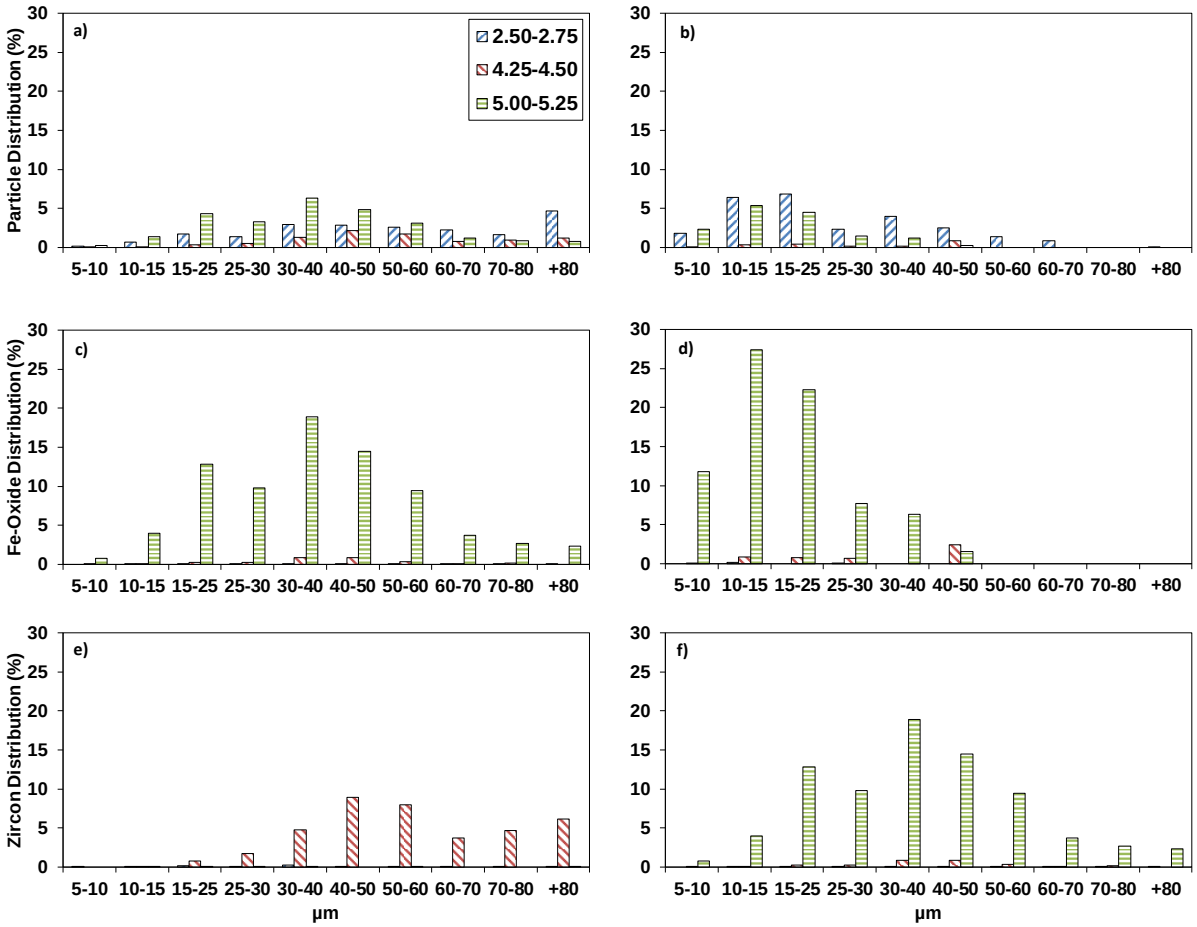

Figure 8 – Distribution of particles (a, b), particles containing iron oxide minerals (c, d) and particles containing zircon (e, f) for three different particle specific gravities across all size classes. Figures on the left (a, c, e) represent the Knelson gravity concentrate and those one the right (b, d, f) represent the Falcon gravity concentrate

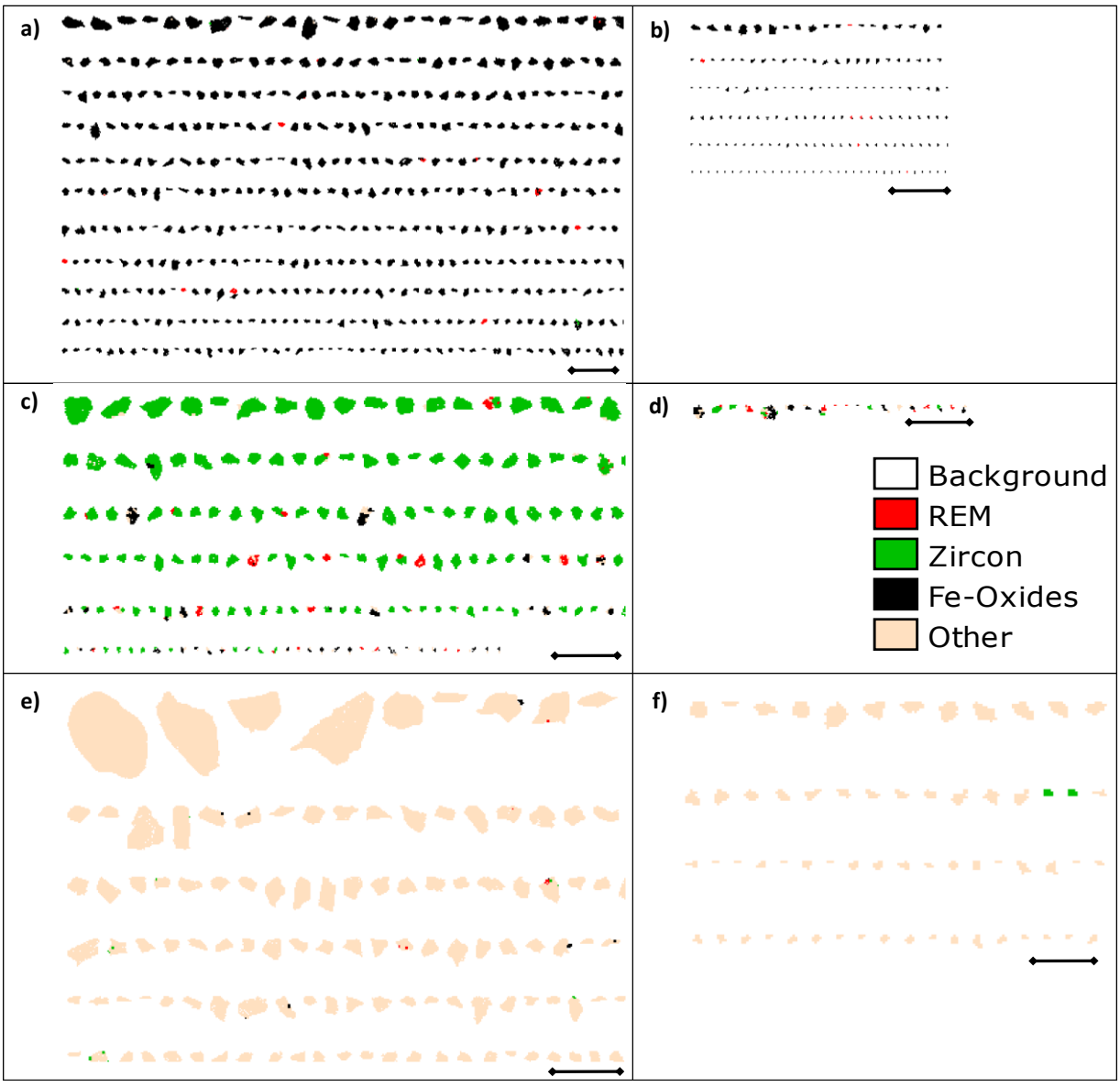

Figure 9 - Particle maps of high specific gravity (5.0-5.25) [a, b], intermediate specific gravity (4.25-4.5) [c,d] and low specific gravity (2.5-2.75) [e,f]. Particle maps on the left (a, c, e) represent the Knelson gravity concentrate and particle maps on the right (b, d, f) represent the Falcon gravity concentrate. Phase identification is limited to four mineral classes: iron oxides, zircon, REM (all other REM) and other (all other mineral phases in the deposit). Scale bars represent 250 µm (a, c, e) and 100 µm (b, d, f)

3.2.2 Deportment of magnetic phases

The choice of magnetic separation steps in this flowsheet (Figure 1) is motivated by the downstream flotation requirement for the rejection of iron-bearing gangue minerals. Additionally, many of the REM in the deposit have been previously determined to be paramagnetic, and thus may possibly be concentrated by a medium intensity magnetic drum separator (Jordens *et al.*, 2014). In order to understand the deportment of magnetic mineral phases in this process, samples from every stream were analysed in a VSM to

determine the magnetism of the sample. This technique, when applied to pure mineral samples, can be used to characterise magnetic properties. VSM results from mixed mineral samples provide general information as to the relative amount of magnetism in a sample. If there is only one main ferromagnetic mineral phase, then the data can be used to indirectly measure the concentration of this magnetic phase. Figure 10 shows VSM results for the feed to the centrifugal gravity and drum magnetic process as well as samples from all process streams. Paramagnetic minerals will have a positive linear slope, while ferromagnetic minerals will show a rapid increase in magnetisation followed by a plateau at the minerals saturation magnetisation (a characteristic property of ferromagnetic materials). A more detailed explanation of mineral magnetism along with VSM measurement of some pure REM is available in Jordens *et al.* (2014).

The coarse fraction of the feed exhibits a lower degree of ferromagnetism (Figure 10a) and indicates that there is either a higher concentration of ferromagnetic minerals or more strongly ferromagnetic minerals present in the finer size fraction. Based on the feed mineralogy (Table 1), the only minerals expected to exhibit ferromagnetic behaviour are the iron oxides (likely a mixture of magnetite and hematite). Based on the similar mineral concentrations (as measured by QEMSCAN) between the size fractions, it can be concluded that the fine (<20 µm) size fraction contains an elevated concentration of a strongly ferromagnetic iron oxide such as magnetite. The results (Figure 10b) show a higher ferromagnetic character for the Knelson gravity concentrate than that in the Falcon gravity concentrate, but both have a higher saturation magnetisation than the feed. The analysis of the two gravity tailings streams (Figure 10c) shows that after gravity separation the remaining mass in the tailings (~90 % of the feed) is most similar in magnetic behaviour to the fine size fraction of the feed. This is intuitive in the context of the results presented in Section 3.2.1 which demonstrated the preferential recovery of coarse particles in the gravity separation step. The results for the magnetic fractions recovered from low intensity magnetic separation (Figure 10d) and medium intensity separation (Figure 10e) show that the Knelson gravity concentrate contains ferromagnetic material, which is primarily recovered at low intensity, while the Falcon gravity concentrate's magnetic products from both low and medium intensity magnetic separation have similar magnetic properties. This is, once again, likely due to particle size effects where the Knelson gravity concentrate contains larger liberated ferromagnetic particles that report to the magnetic fraction of a wet drum magnetic separator at lower applied magnetic field strengths. This is confirmed by the iron oxide mean grain sizes calculated from QEMSCAN, which show the low intensity and medium intensity magnetic fractions from the Knelson gravity concentrate are larger (32 and 26 µm, respectively) than those produced from the Falcon (15 and 14 µm, respectively). Figure 10f shows a lack of ferromagnetism indicating that both non-magnetic products from medium intensity wet drum magnetic separation have very low concentrations of strongly ferromagnetic iron oxide minerals.

If the oversimplification of treating all samples in this flowsheet as binary mixtures of a paramagnetic mineral and a ferromagnetic mineral is made, then it is possible to semi-quantitatively evaluate and compare the ferromagnetic mineral content of each sample using Honda-Owen analysis. This analysis is more typically used in the elimination of the effects of a ferromagnetic impurity from VSM data for a paramagnetic sample (Jordens *et al.*, 2014). Table 2 shows the results of this analysis assuming magnetite is the lone ferromagnetic mineral in the deposit. Although this might be incorrect it does provide a means of quantitatively comparing the VSM results.

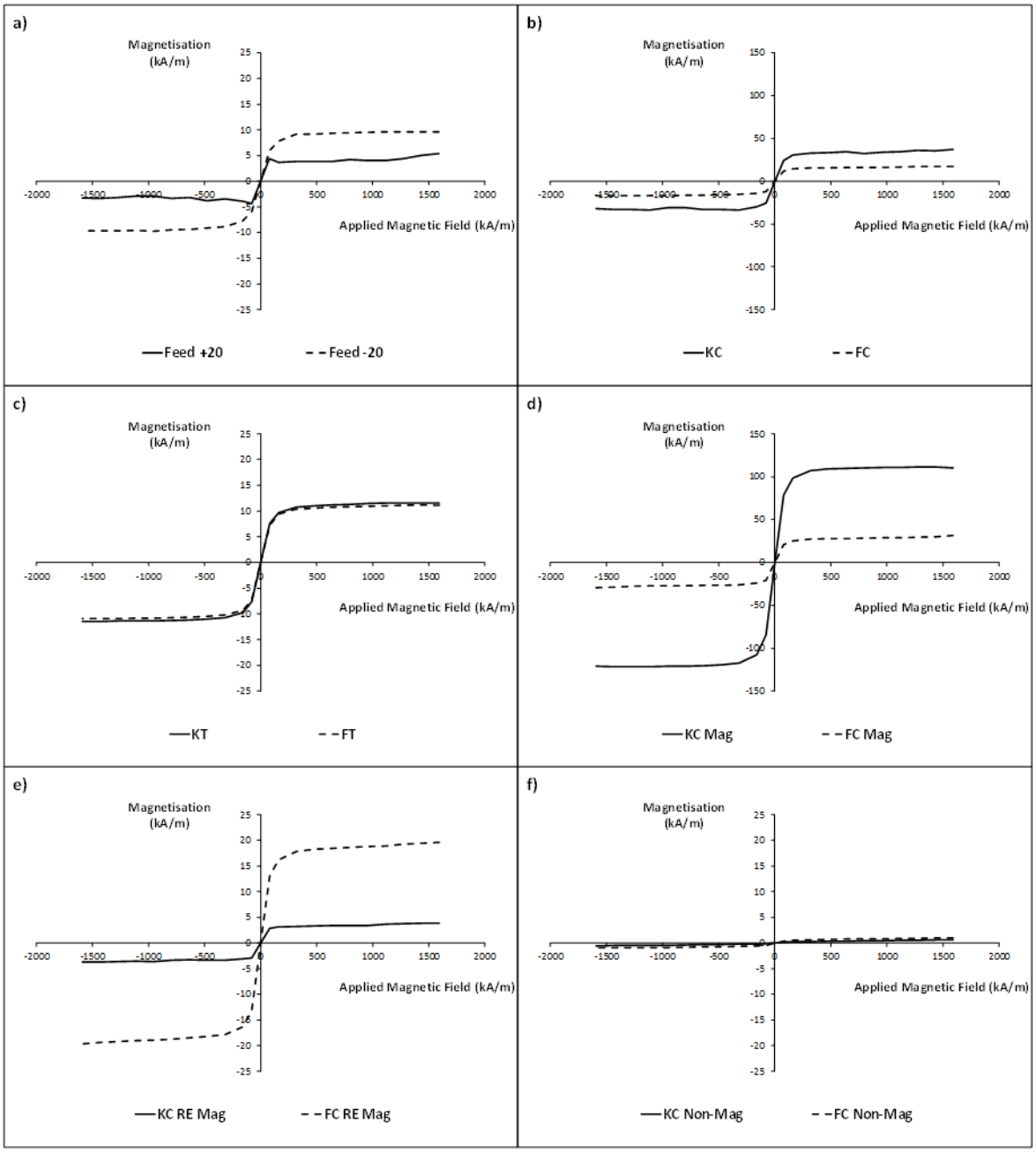

Figure 10 – Magnetic behaviour (magnetisation as a function of applied magnetic field) of samples from centrifugal gravity + wet drum magnetic flowsheet as determined by VSM for: a) feed, b) gravity concentrates, c) gravity tailings, d) low intensity magnetic fraction, e) medium intensity magnetic fraction, f) non-magnetic fraction

Table 2 – Calculated magnetite content of different separation products from Honda-Owen analysis of VSM data

Stream Designation	Calculated Magnetite Content (%)
Feed +20	0.75
Feed -20	1.95
KC	6.70
FC	3.17
KT	2.33
FT	2.22
KC Mag	23.24
KC RE Mag	0.62
KC Non-Mag	0.00
FC Mag	5.59
FC RE Mag	3.74
FC Non-Mag	0.12

3.2.3 Grade and recovery of REM

Size-by-size recoveries of zircon, LREM and iron oxides are shown in Figure 11 (due to low concentration and small grain sizes, data for fergusonite and columbite were excluded from this analysis). It can be seen from Figure 11 (a, b) that coarse zircon recovery occurs exclusively in the Knelson Concentrator while the Falcon Concentrator recovers fine-grained light REM (Figure 11 (c, d)). Recovery of coarse iron oxides occurs in the Knelson, while fine grained iron oxide in the Falcon shows higher recovery (Figure 11 (e, f)). For the Knelson gravity concentrate, the low intensity magnetic fraction has the highest recovery of iron oxides while the non-magnetic product from medium intensity magnetic separation contains the highest recoveries of zircon (Figure 11a and to Figure 11e). This suggests that the wet drum magnetic separation is efficiently rejecting iron oxide minerals which are collected in the gravity separation stage.

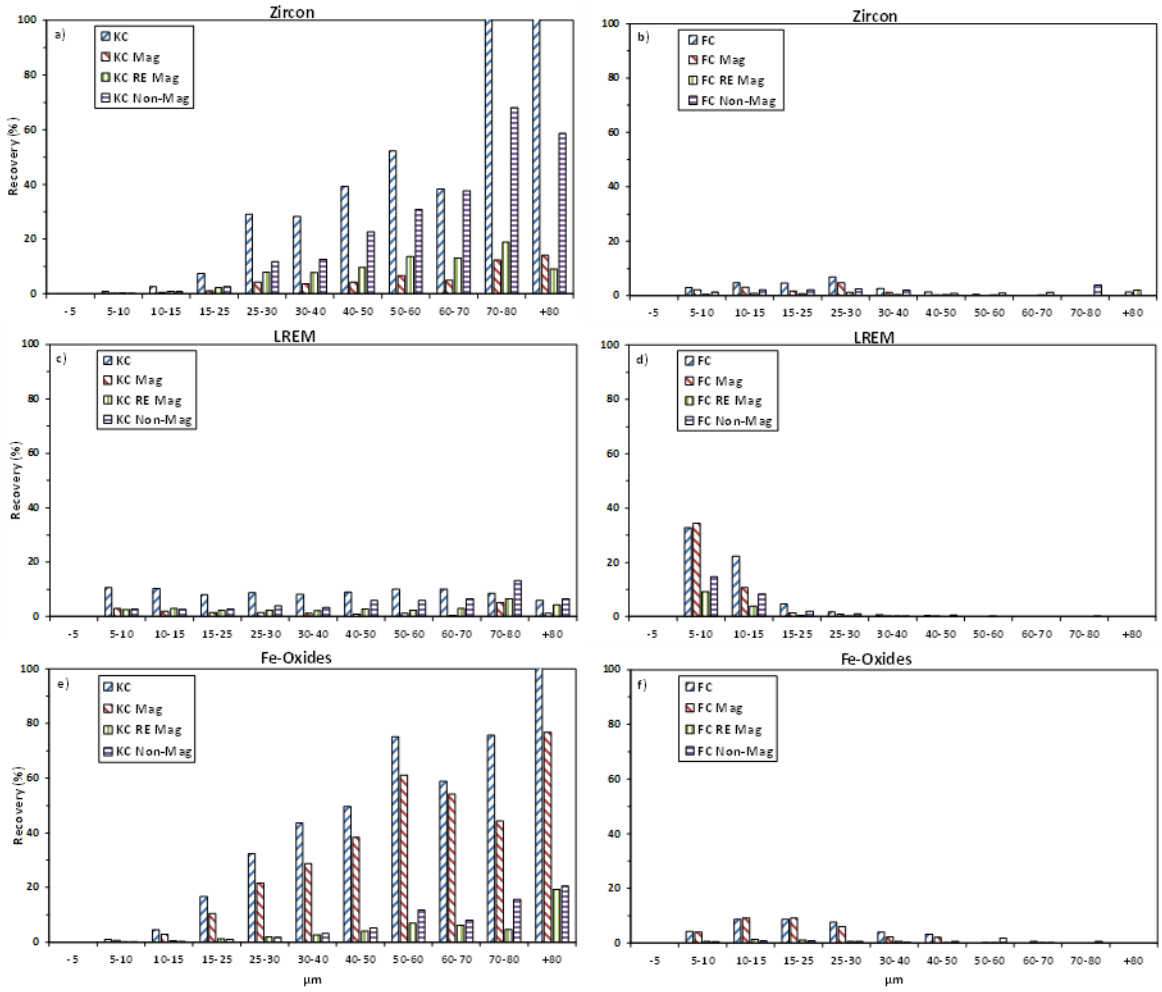

Figure 11 – Size-by-size recoveries of: zircon (a, b), LREM (c, d) and iron oxide minerals (e, f). The left column represents the Knelson gravity concentrate and associated downstream magnetic separation products while the right represents the Falcon gravity concentrate and associated downstream magnetic separation products

Mineral and elemental grade and recovery results were reported for these separations in (Jordens *et al.* (2015), Section 3.2.2). A further discussion of the optimum fraction for downstream flotation is presented in Section 3.5.

Scanning electron microscopy and energy dispersive X-ray spectroscopy were used to qualitatively identify important elements (Zr, Fe, La, Ce, Nd, and Y) as well as REM in the feed (Figure 12) and products of gravity (Figure 13) and magnetic separation (Figures 14 and 15). While SEM images provide only qualitative information they are an important empirical check against automated mineralogical techniques which assign mineral chemistry based on a mineral definition database. For example the upper left image in Figure 13 clearly shows Y found alongside Zr, verifying that recovering the zircon mineral results in recovery of HREE such as Y. The SEM images in Figures 12 and 13 illustrate the differences between the Knelson and Falcon gravity concentrates in terms of particle size as well as demonstrating the successful concentration of Zr, Fe and REM into the gravity concentrates. The images of the products of magnetic separation of the Knelson gravity concentrate (Figure 14) show that fine Fe particles are concentrated into the low-intensity magnetic product with coarse REM remaining in the medium-intensity magnetic and non-magnetic

products. Figure 15 shows a similar trend for the recovery of REM in the non-magnetic fractions of the Falcon gravity concentrate, but the removal of Fe-bearing minerals occurs over both low-intensity and medium-intensity magnetic products.

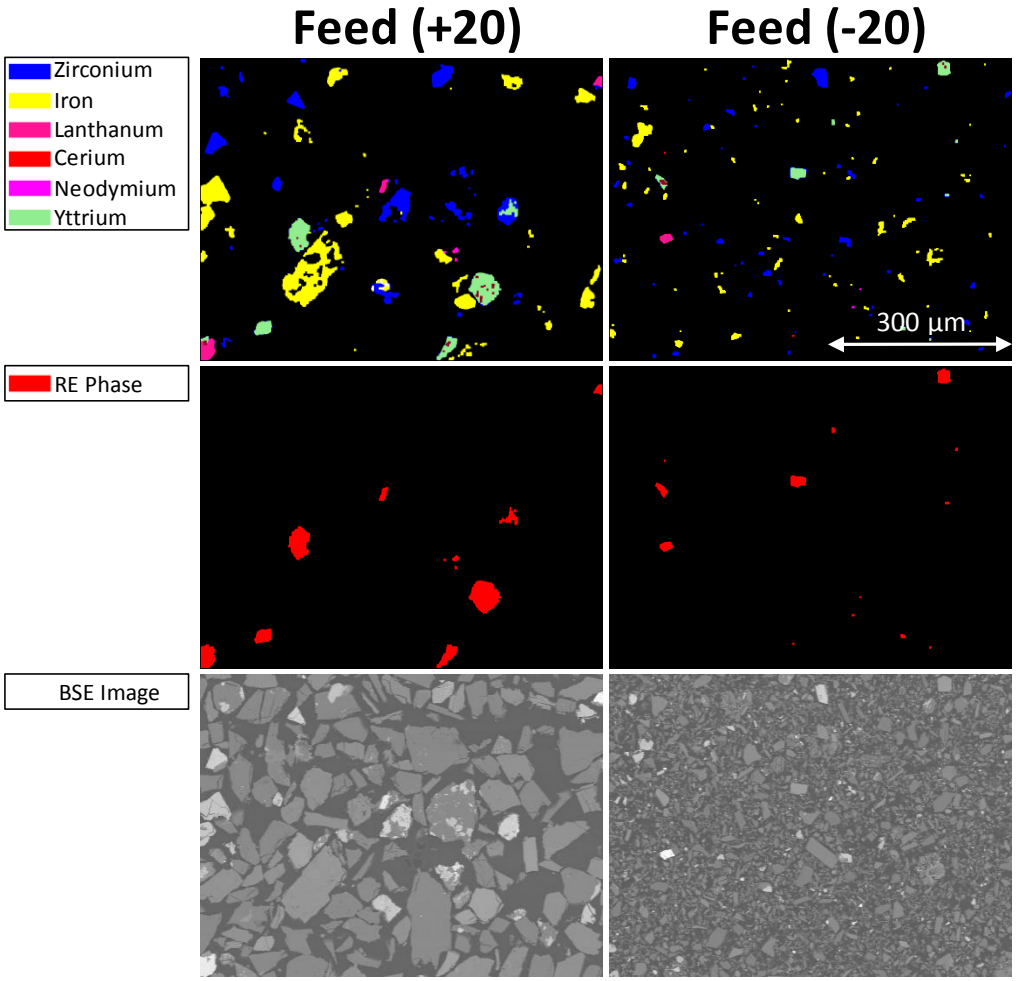

Figure 12 – SEM images of the feed (+20 µm and -20 µm) to gravity and magnetic separation including elemental (Zr, Fe, La, Ce, Nd, Y) phase identification, REM phase identification and backscattered electron (BSE) images

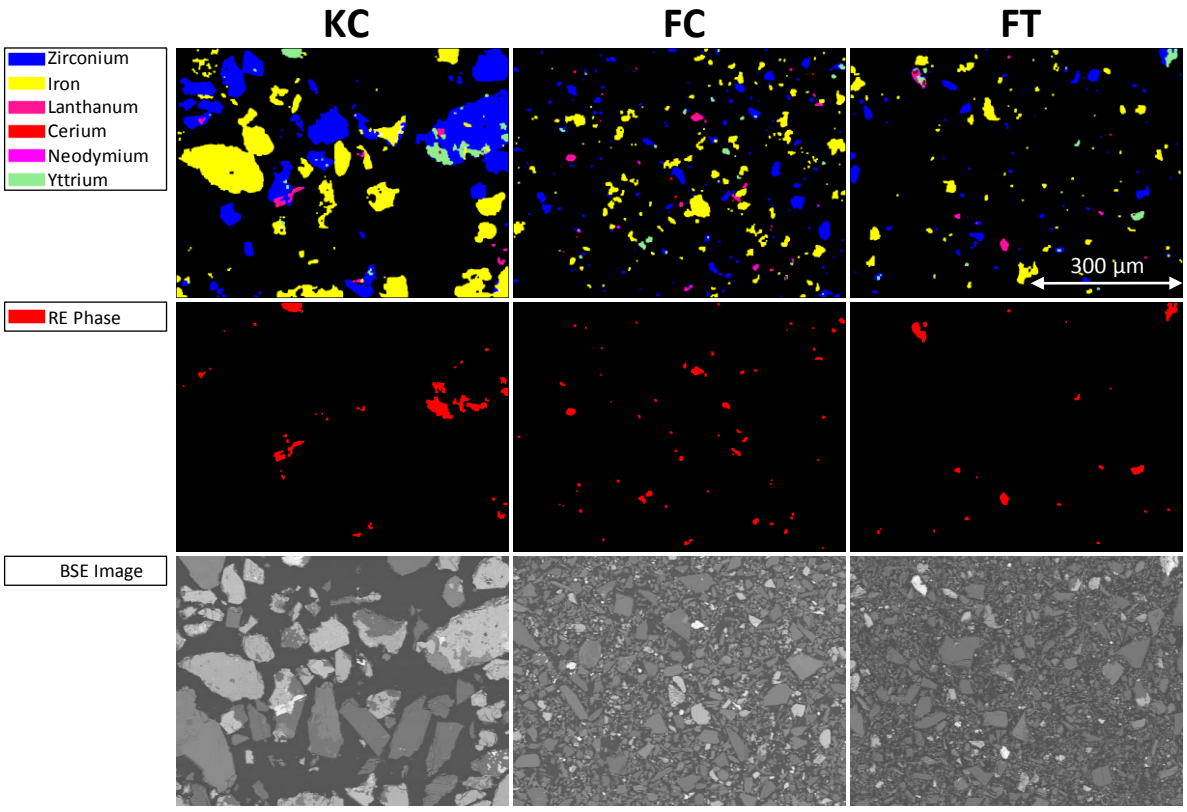

Figure 13 – SEM images of the Knelson Con (KC), Falcon Con (FC) and Falcon Tailings (FT) including elemental (Zr, Fe, La, Ce, Nd, Y) phase identification, REM phase identification and backscattered electron (BSE) images

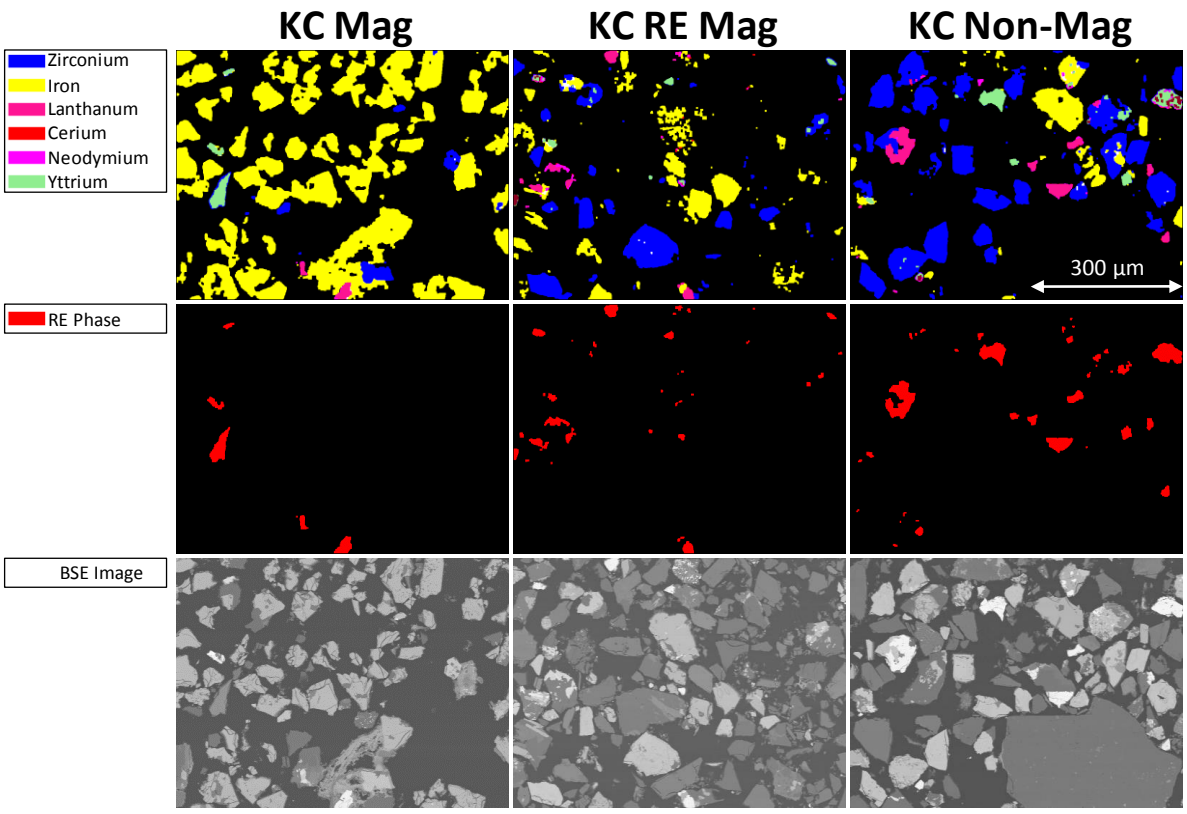

Figure 14 – SEM images of the Knelson Con low intensity magnetic product (KC Mag), Knelson Con medium intensity magnetic product (KC RE Mag) and Knelson Con non-magnetic product (KC Non-Mag) including elemental (Zr, Fe, La, Ce, Nd, Y) phase identification, REM phase identification and backscattered electron (BSE) images

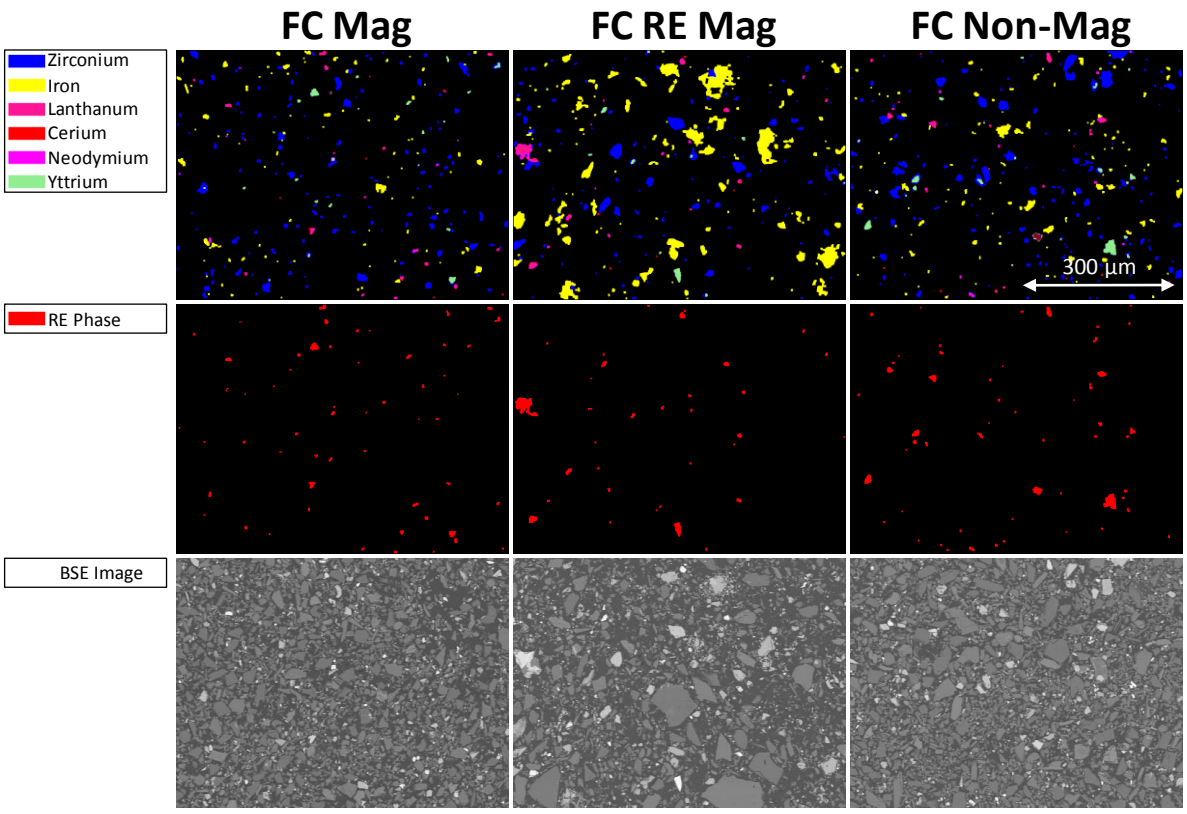

Figure 15 – SEM images of the Falcon Con low intensity magnetic product (FC Mag), Falcon Con medium intensity magnetic product (FC RE Mag) and Falcon Con non-magnetic product (FC Non-Mag) including elemental (Zr, Fe, La, Ce, Nd, Y) phase identification, REM phase identification and backscattered electron (BSE) images

3.3 Selection of optimal fraction for downstream processing

The ultimate goal of the processes presented in Sections 3.2 and Jordens *et al.* (2015) was to produce a product for downstream froth flotation. The requirements for this product include: rejection of iron-bearing gangue (detrimental to flotation with hydroxamates); rejection of silicate gangue and maximizing the grade and recovery of REE, in particular the heavy REE which have the greatest economic impact to a potential REE mine. In order to combine mineralogical and elemental grade and recovery data for many different minerals and elements and many different product streams, graphs of upgrade ratio versus recovery were created. On such a graph, different minerals from the same sample will form a linear line with the length of the line between points indicating the selectivity of that sample for one mineral (or group of minerals) over another. The point at the upper right of such a graph is the mineral which is being concentrated to the greatest extent and the point at the lower left is the mineral being rejected to the greatest extent. Upgrade ratio is a better indicator than grade as the change in grade may not be indicative of the degree to which a given mineral is concentrated if the initial concentration of the mineral is relatively low.

Graphs of upgrade ratio versus recovery were created for the streams produced from centrifugal gravity concentration and wet drum magnetic separation (Figure 16 (a, b)); for different combinations of these product streams such as the combined magnetic fractions from low intensity drum magnetic separation (Mags); the combined magnetic fractions from medium intensity drum magnetic separation (RE Mags); the

combined non-magnetic fractions from medium intensity drum magnetic separation (Non-Mags); and several others (Figure 16 (c, d)).

Figure 16a illustrates that the centrifugal gravity concentration steps preferentially upgrade iron oxides, and that those iron oxides are even further upgraded by low intensity magnetic separation. The non-magnetic fractions from the medium intensity magnetic separation are enriched in zircon and other REM, while the magnetic fractions from medium intensity magnetic separation of the Falcon gravity concentrate is actually enriched with iron oxides (Figure 16b). This suggests that the medium intensity magnetic separation may only be necessary to remove iron oxide minerals from the Falcon gravity concentrate stream. Figure 16c shows combinations of these streams, with the Mag product showing the best upgrade ratio and recovery of iron oxide minerals while the RE Mag + Non-Mag shows the best results for zircon and REM. Several other combinations of the RE Mag and Non-Mag streams are shown in Figure 16d, where it can be seen that a combination of the RE Mag and Non-Mag streams from the Falcon gravity concentrate offers very low recoveries and upgrade ratios. The other three stream combinations are very difficult to differentiate.

As one of the criteria for the final fraction from this process is to maximize the recovery of HREE, graphs of elemental upgrade ratio versus recovery are shown in Figure 17 for the four stream options selected from Figure 16 with the best REM upgrading and recovery. The results show that all four options considered preferentially concentrate the HREE with the Non-Mag (KC) stream providing the highest upgrade ratio and the combination of all RE Mag and Non-Mag streams providing the highest recovery values.

The final decision on which fraction to carry forward for downstream flotation is based on two factors: maximizing both REO grade and recovery; and avoiding an unnecessarily complex physical separation process. For this reason the RE Mag and Non-Mag fractions from the Knelson gravity concentrate were selected as the feed to downstream flotation processes as this achieves a high upgrade ratio (Figure 17b) while also eliminating everything but the Knelson Concentrator and low intensity wet drum magnetic separation process steps from the initially investigated process flowsheet (Figure 1).

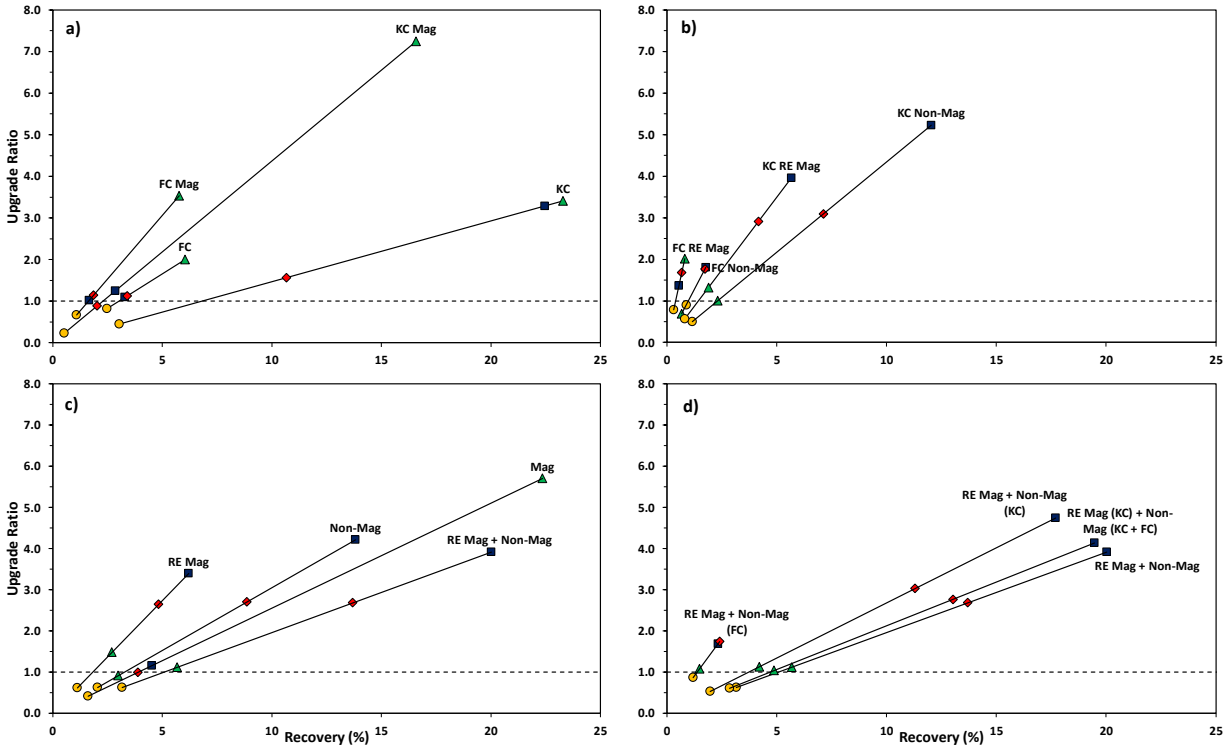

Figure 16 – Upgrade ratio versus recovery as determined by QEMSCAN for different product streams and combination of product streams: a) gravity concentrates and low intensity magnetic fractions, b) medium intensity magnetic and non-magnetic fractions, c) combinations of low intensity magnetic, medium intensity magnetic and non-magnetic product streams, d) alternate combinations of the non-magnetic products from low intensity magnetic separation. In each figure the symbol represents the upgrade ratio and recovery of: zircon [squares], all other REM [diamonds], iron oxide minerals [triangles] and silicate gangue (quartz, K-feldspar, plagioclase and biotite) [circles]

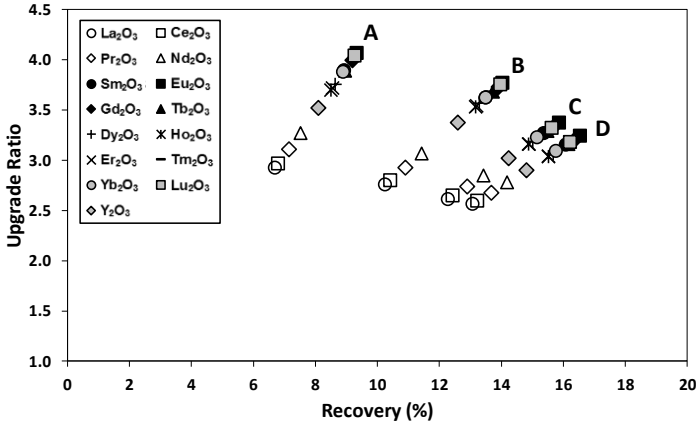

Figure 17 – Upgrade ratio versus recovery for individual REO as determined by ICP-MS: a) Non-Mag (KC), b) RE Mag + Non-Mag (KC), c) RE Mag (KC) + Non-Mag (KC + FC), d) RE Mag + Non-Mag.

Similar graphs of upgrade ratio versus recovery were also created for the oversize material screened from the Knelson gravity concentrate (Figure 18). It is interesting to note that a simple gravity concentration step applied to very coarse particles in the feed material is able to produce upgrade ratios between 2 and 3 for zircon (although at very low recoveries). A particle map of this oversize material sorted by particle size and calculated particle specific gravity similar to Figure 9 was created and is shown in Figure 19. It can be seen visually in this figure that the particles in the Knelson gravity concentrate oversize fraction with specific gravities between 3.25 and 4.5 are enriched in the zircon mineral phase across a wide size range. This suggests that grain size differences in the deposit may present opportunities for selective comminution.

An expansion of this work to develop a stage grinding, gravity and magnetic separation circuit could include a grind to a much coarser particle size (~300 microns) followed by a centrifugal gravity concentration step, followed by further grinding of the gravity concentrate, with a final low intensity magnetic separation step to separate coarsely liberated iron oxide minerals from the enriched REM fraction. Such a flowsheet, while not suitable for processing the entire Nechalacho deposit, could present opportunities to minimise grinding costs while producing an initial high grade REM concentrate for hydrometallurgical processing or as part of a pre-concentration process prior to REM flotation. Such a process could certainly be expected to be easier to commission in an industrial setting than novel REM flotation schemes which typically include reagents with minimal in-plant testing and validation. The proposed process would be analogous to the use of centrifugal gravity concentration in gold processing flowsheets to target gravity recoverable gold recovery initially during plant startup and commissioning to provide an early revenue stream, and thereby improve project economics.

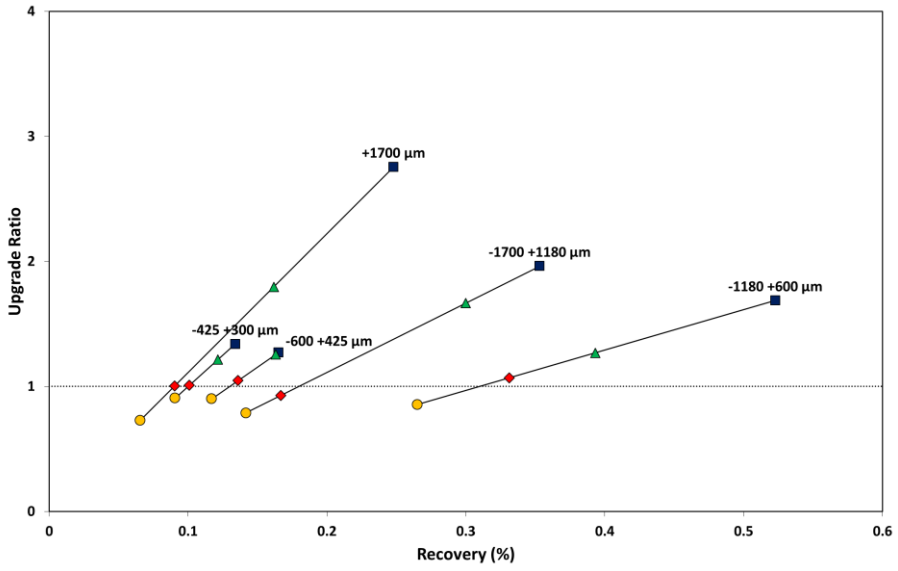

Figure 18 – Upgrade ratio versus recovery as determined by QEMSCAN for different size fractions of the Knelson gravity concentrate oversize material. In each figure the symbol represents the upgrade ratio and recovery of: zircon [squares], all other REM [diamonds], iron oxide minerals [triangles] and silicate gangue (quartz, K-feldspar, plagioclase and biotite) [circles]

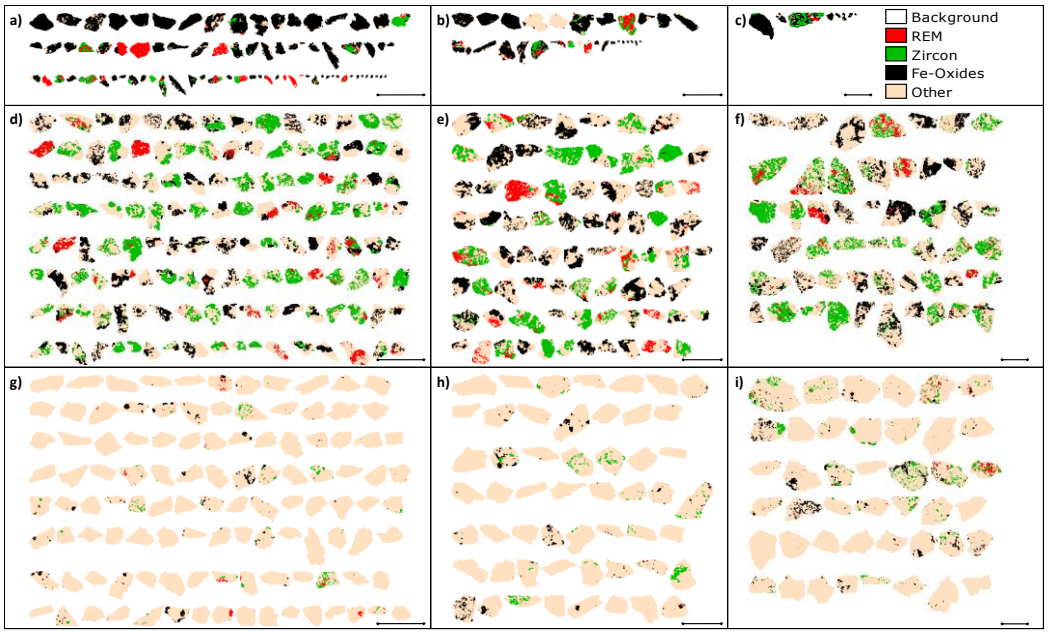

Figure 19 - Particle maps of high specific gravity (> 4.5) [a, b, c], intermediate specific gravity (3.25-4.5) [d, e, f] and low specific gravity (2.5-3.25) [g, h, i]. Particle maps on the left (a, d, g) represent the 300-425 µm fraction of the Knelson gravity concentrate, particle maps in the middle of the figure (b, e, h) represent the 425-600 µm fraction of the Knelson gravity concentrate, and particle maps on the right (c, f, i) represent the 600-1180 µm fraction of the Knelson gravity concentrate. Phase identification is limited to four mineral classes: iron oxides, zircon, REM (all other REM) and other (all other mineral phases in the deposit). Scale bars represent 1 mm

4. Conclusions

This paper described the mineralogical characterisation of the products from gravity and magnetic separation steps applied to a REM feed from the Nechalacho deposit (Northwest Territories, Canada). Characterisation of the product streams using QEMSCAN, SEM and VSM measurements allowed the following conclusions to be made:

- REM recovery from this deposit using centrifugal gravity concentration is effective although recovery decreases with decreasing particle size
- The Knelson Concentrator in this process exhibited greater selectivity for particle size and particle specific gravity compared to the Falcon Concentrator. This may be due to the lack of fluidizing water in the Falcon (different bowl geometry), higher centrifugal accelerations experienced by the particles or the different distribution of mineral particles fed to the Falcon as opposed to the Knelson
- The oversize material in the Knelson gravity concentrate is enriched with zircon, suggesting that a coarser initial grind size should be investigated with centrifugal gravity separation and low intensity magnetic separation to produce a heavy REE-enriched concentrate
- The optimal fraction from this process to send to a downstream flotation stage is the non-magnetic fraction left after low intensity wet drum magnetic separation of the Knelson gravity concentrate with a total RE oxide (TREO) recovery of 11.75 % and a grade of 7.50 % TREO, 10.69 % iron oxides and, 35.80 % silicates (quartz + feldspar)
- It is important to note that this process is not representative of the currently selected process design or recovery for the Nechalacho deposit. Any application of this process to this deposit would require optimisation in order to ensure appropriate grade and recovery targets are met

Acknowledgements

The authors would like to acknowledge funding from the Natural Sciences and Engineering Research Council of Canada (NSERC) and Avalon Rare Metals for providing funding for this work through the Collaborative Research and Development (CRD) Program (444537-12). The authors also acknowledge funding for A. Jordens from the McGill Engineering Doctoral Award as well as an NSERC Alexander Graham Bell Canada Graduate Scholarship, and funding for C. Marion from the McGill Engineering Doctoral Award as well as an NSERC CGS M award. The authors acknowledge the assistance of J. Helal and S. McCarthy in conducting some of the gravity separation and specific gravity measurement experiments, respectively. The authors also acknowledge SGS Canada Inc. for offsetting some of the costs of QEMSCAN analysis in this work.

References

Grammatikopoulos, T., Mercer, W. and Gunning, C. (2013). Mineralogical characterization using QEMSCAN of the Nechalacho heavy rare earth metal deposit, Northwest Territories, Canada. *Canadian Metallurgical Quarterly*, **52** (3): 265-277.

Horny, P., Lifshin, E., Campbell, H. and Gauvin, R. (2010). Development of a new quantitative X-ray microanalysis method for electron microscopy. *Microscopy and Microanalysis*, **16** (6): 821-830.

Jordens, A., Marion, C., Langlois, R., Grammatikopoulos, T., Rowson, N.A. and Waters, K.E. (2015). Beneficiation of the Nechalacho Rare Earth Deposit. Part 1: Gravity and Magnetic Separation. *Minerals Engineering (submitted)*.

Jordens, A., Sheridan, R.S., Rowson, N.A. and Waters, K.E. (2014). Processing a rare earth mineral deposit using gravity and magnetic separation. *Minerals Engineering*, **62**: 9-18.

Pascoe, R.D., Power, M.R. and Simpson, B. (2007). QEMSCAN analysis as a tool for improved understanding of gravity separator performance. *Minerals Engineering*, **20**: 487-495.